Innovative application of Nile Red (NR)-based dye for direct detection of micro and nanoplastics (MNPs) in diverse aquatic environments

Graphical Abstract

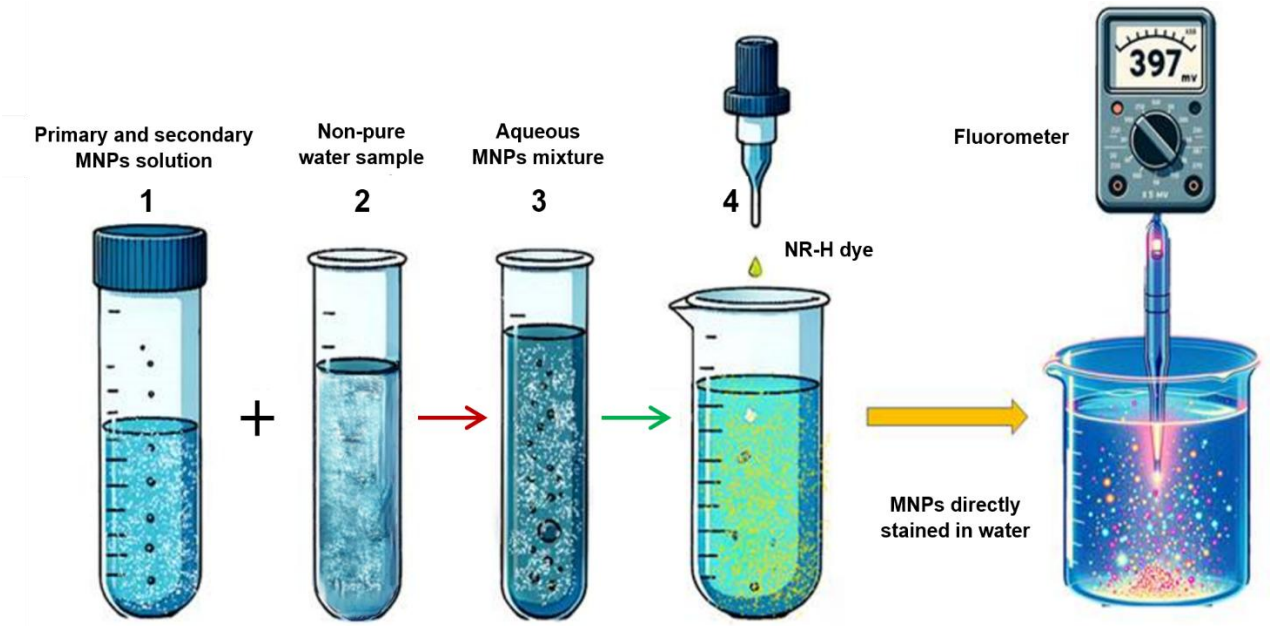

Abstract

This paper presents the results of a research aimed at establishing a novel method for the detection of primary and secondary micro- and nanoplastics (MNPs), by using the fluorescence properties of the dye Nile Red-n-heptane (NR-H). The method has been applied to the detection of laboratory degraded polymers (Polystyrene, PS and Polyethylene Terephthalate, PET) as well as traceable latex microspheres in aqueous environments, showing a remarkable detection capacity and avoiding the prior extraction or processing of MNPs in natural samples, with significant time savings compared to conventional methods. The study has been carried out on various types of water, including samples from wastewater treatment plants, boreholes, seawater and synthesized

seawater. The effectiveness of the staining process was evaluated by scanning electron microscopy (SEM), dynamic light scattering (DLS) and optical microscopy. As a result, a novel standardizable protocol for the rapid detection of MNPs has been established, with the potential to improve environmental protection through fast in-situ detection and identification of plastic contaminants. The limitations of the protocol in the quantification of MNPs have also been identified and further studies are proposed to overcome these limitations.

Keywords: Microplastics; nanoplastics; Nile Red staining; environment; fluorescence-fluorometry.

1. Introduction

The rising issue of plastic waste, particularly from prevalent single-use products, is alarming from an environmental point of view (Ibrahim et al., 2024), with projections indicating that plastic waste in the EU-27 could skyrocket to 17 million tons per year by 2030 (Fan et al., 2022).This situation is exacerbated by environmental factors like ultraviolet (UV) radiation, oxidation, temperature fluctuations mainly (El Hadri et al., 2020), which combined lead to the breakdown of larger plastics, like bottles, into minuscule fragments termed as microplastics and nanoplastics (MNPs), depending on the resulting sizes (0,1 to 3000 m for microplastics, while particles from 1 to 100 nm are considered nanoplastics). Both types of MNPs (Frias & Nash, 2019; Gonçalves & Bebianno, 2021; Toussaint et al., 2019) , that intentionally manufactured for their industrial use (primary MNPs) or those resulting from natural degradation of original plastics (secondary MNPs), present substantial ecological dangers and pose serious threats to human health, owing to their ability to permeate food chains (Brennholt et al., 2018; Koraltan et al., 2022).

Addressing this multifaceted problem requires innovative, precise, and reliable detection and quantification methodologies. Recent studies (Alvim et al., 2023; Jiménez-Lamana et al., 2023; Pradel et al., 2022) made significant strides in this area, proposing new techniques and approaches using diverse plastic polymers, including varieties like polyethylene (PE), polypropylene (PP), polystyrene (PS), polycarbonate (PC) among others which necessitates a range of methodological approaches for effective analysis. This complexity is particularly evident in aquatic ecosystems, with specific characteristics of various sample types, including drinking water, natural watercourses, foods, sediments, biota tissues, and wastewater treatment plant outputs (Burzio et al., 2022; Tröger et al., 2018). Samples with high organic content may require prior digestion using acidic, alkaline, or enzymatic methods, while simpler samples like drinking water might only necessitate preconcentration. In scenarios involving organic solvents, evaporation techniques, as rotary evaporators under reduced pressure, are commonly used. These specific methods are essential to accurately analyze the wide variety of plastic polymers (Myszograj, 2020) present in different aquatic environments.

For detecting MNPs, several advanced technologies are employed (Lee & Chae, 2021; Shruti et al., 2021). These serve for different purposes: separate and concentrate the raw sources to make easier the MNP´s detection (Ibrahim et al., 2024; Rezania et al., 2018); detect their presence and characterize them; and finally, identify which plastic molecules comprise the MNP´s. Main techniques used for these purposes are summarized in Fig. 1. These include Scanning (SEM) and Transmission (TEM) Electron Microscopy for detailed morphological analysis, as well as Fourier-Transform Infrared Spectroscopy (FTIR) and Raman Spectroscopy (Zhang et al., 2023) for MNPs chemical characterization and identification (Campo et al., 2019; Tirkey & Upadhyay, 2021). Additionally, other analytic methods like Pyrolysis-Gas Chromatography/Mass Spectrometry (Py-GC/MS) and Dynamic Light Scattering (DLS) contribute to a detailed picture of MNPs' compositions, sizes, and degradation patterns. Initial

segregation of plastic fragments is done using a down to millimeter sieve. For particles under 1 µm, two separation techniques are utilized: active field flow fractionation (FFF) for complex environments and passive hydrodynamic chromatography (HDC) based on controlled pore sizes. Nanoparticle tracking analysis (NTA) assesses particle concentrations in aqueous suspensions by analyzing, frame-by-frame, Brownian motion. Furthermore, flow cytometry (FCM) and hyperspectral imaging (HSI) are used for counting MNPs in fluid flows by detecting reflected light from particles.

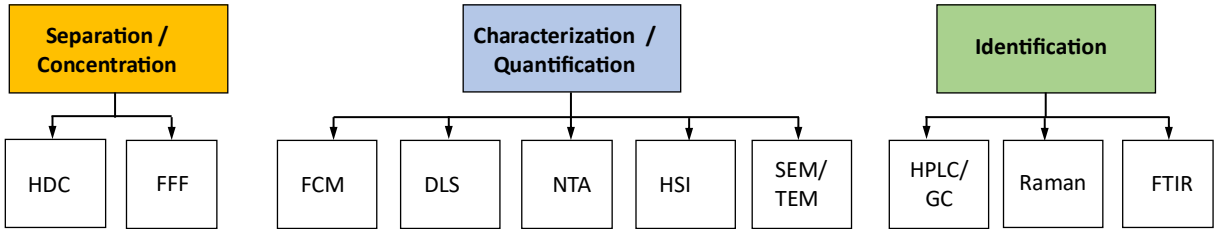

Fig. 1. Overview of methods for the separation, characterization, and identification of Microplastics and Nanoplastics in Aquatic Environments.

Among those methods, fluorescence is very commonly used in MNPs detection, characterization and identification. In that sense, Nile Red (NR), a lipophilic fluorescent dye, has become a prominent tool, particularly in distinguishing various polymer types in environmental samples. Introduced by Andrady (Andrady, 2011 and 2017) and validated in numerous studies (Alvim et al., 2023; Bianco et al., 2023; Gagné et al., 2019; Hernández et al., 2023; Nalbone et al., 2021; Shim et al., 2016; Sturm et al., 2023) NR's application involves staining microplastics for visualization under a fluorescence microscope. This technique surpasses traditional optical microscopy in specificity, aided by NR's hydrophobic properties, making it an asset in MNP's identification for polymers like PE, PP, EPS, PS, and others. NR hydrophobic interactions and dynamic fluorescence modulation, ensure a strong affinity to non-polar regions of polymers (Sturm et al., 2021, 2023). Employing NR in MNP detection involves

dissolving it in organic solvents to maximize its molecular interactivity, revealing MNP's in diverse environmental matrices. The dye's interaction mechanisms, offer a comprehensive detection approach that is both user-friendly and cost-efficient, even with portable fluorescence imaging tools (Prata et al., 2021).

However, the use of fluorescence-based methods, as in general, any other method used to identify the presence of MNP's requires a previous preparation of the sample in which we wish to detect the presence of these contaminants. In general, this stage consists of filtering the sample through a suitable membrane that collects possible contaminants, and then applying the staining process and subsequent detection to the result. This obviously slows down the detection process, which also needs to be carried out in a separate laboratory, where the necessary filtration and fixation equipment is available, thus avoiding the possibility of a rapid in-situ control of the presence of MNPs. In order to overcome this problem, the main objective of this work is to develop an experimental protocol based on NR staining of MNPs present in water samples in order to directly and rapidly detect the presence of these contaminants.

To achieve this objective, we will start by studying the fluorescent properties of NR, in order to obtain the optimal conditions for the preparation of the dye so that the resulting fluorescence signal is maximized. We will then test the functionality of the optimized dye against test solutions in pure water. In one solution, primary MNPs (modelled in this case by using calibrated latex particles with a narrow size distribution) will be used. In the other pure water solution, secondary MNPs generated in our laboratory from PS and PET will be tested. The choice of calibrated latex particles as primary NPM models is based on several advantages, including the fact that they are readily available in the desired sizes, making it easy to model their behavior in many types of studies. However, they also have certain limitations, which need to be known, in terms of their behavior in terms of dispersion, aggregation kinetics and

sedimentation patterns in water, so that they may differ from real primary MNPs (Gigault et al., 2021; Reynaud et al., 2022; Gigault et al., 2018).

On the other hand, alongside the latex particles used for calibration and validation purposes, secondary MNPs were obtained following a slow controlled degradation protocol. These particles were subsequently used to test the efficacy of the proposed identification method. As a final step of this study, the use of the NR-H staining protocol for the detection of MNPs in water samples from various natural sources was analyzed. The aim of this part of the study was to check whether the protocol developed was suitable for the detection of MNPs in possibly contaminated water, where there was a possibility of cross-interactions of the dye with other non-plastic contaminants, so that the detection of real MNPs would be masked or minimized. To this end, the protocol was adapted for use with water from different sources, rich in dissolved organic and inorganic matter (sediments, nutrients, solids, biofilms, pathogens, chemicals, minerals, salts...) to which our primary and secondary MNPs were added, and the detection response was tested.

This study aims to facilitate the rapid and direct detection and characterization of MNPs, eliminating the need for laborious sample preparation procedures. However, the work presented here, as an initial step in a more in-depth investigation, is being continued with a view to determining the possibilities of this protocol for the quantification of the MNPs present in the samples (an objective that was not addressed in this study), as well as verifying its usefulness in the presence of other types of MNPs commonly found in the polluted waters of our seas and rivers.

2. Materials and methods

2.1. Primary MNPs

For protocol calibration, we employed NIST® (National Institute of Standards and Technology) traceable latex beads procured from Thermo Scientific. These beads are dispensed in dropper-tipped bottles containing 15 ml to ensure precise volumetric delivery and minimize operator variance, thereby enhancing reproducibility. Recognized for their uniformity, stability, and accessibility, these beads are exemplary for instrument calibration. Their meticulously characterized dimensions and near-perfect sphericity render them ideal as surrogates for primary plastics in our studies. We selected beads spanning a size range from 100 μm down to 0.05 μm to cover a broad spectrum of particulate dimensions.

2.2. Secondary MNPs

In this study, secondary MNP's were generated from polystyrene (PS) packaging lids often used in packaging protection and delivery. The pieces of PS lids were broken off resulting in a set of small beads, each with a diameter of approximately 1 to 3 mm, with an aggregate weight of 500 grams. Subsequently, the PS beads were placed in an empty, dry water bottle (made of PET) and the bottle was filled up to 5 liters of capacity with ultra-pure water.

The bottle containing the PS beads was placed in a weathering chamber (manufactured by Binder GmbH), where it was subjected to accelerated and controlled degradation for 1 year. For this purpose, the temperature in the chamber was kept at 35 °C and the container was illuminated with UV light (320-400 nm) for 12 h every day, in order to mimic the degrading effects of sunlight. Every 10-day, a part of the stored water was siphoned off and passed through a Teflon membrane (Sartorius, 100 μm nominal pore), to prevent any external contamination that might transpire due to degradation. The filtered water was then returned to its PET vessel.

After a complete year of systematic degradation, Nanoparticle Tracking Analysis (NTA) technique (NanoSight from Malvern Scientific) and Micro Fourier Transform Infrared Spectroscopy (μFTIR), by means of a Buker Alpha (E-103) instrument, were employed to

check resulting MNP´s. 10 ml aliquots extracted from degraded reservoir, as well as control and blank sets, were analyzed using NTA's software to check plastic concentration in the final water (big amounts of MNP´s was found with concentration ranging from 10^7 to 10^{12} particles/mL depending from zones of the reservoir). Finally, secondary MNPs were subjected to μFTIR analysis, conducted in the range of 4000 to 600 cm^{-1} (resolution $\Delta k = 4$ cm^{-1}). Subsequently results were compared with reference materials. Additionally, carbonyl index (CI) and methyl index (MI) were calculated.

2.3. Nile Red (NR) dye solution

In MNPs detection by using NR-fluorescence, dye solvents as acetone, hexane, and heptane can be selected to optimize dye performance (Shim et al., 2016). The NR's solvatochromism implies resulting color changes in response to different solvents (Maes et al., 2017), allowing Nile Red to produce distinct colors for diverse polymers. In our case, we decided to dissolve NR in acetone to enhance solving, and then adding this solution to n-heptane which serves as a vehicle for staining MNP´s in water. For our experiments, we acquired NR powder (C20H18N2O2 > 95.0%), acetone (99% purity) and n-heptane (purity > 98%), all of them acquired from Thermo Fisher, and used as received.

Initially, Nile Red (NR) dye was dissolved to a concentration of 1 mg/mL in acetone, a polar solvent, to prepare the stock solution. Subsequently, we developed a specialized fluorochrome, NR-Heptane (NR-H), by incorporating n-heptane as an additional solvent. n-Heptane, a non-polar solvent, enhances the solubility of the hydrophobic Nile Red due to its non-polarity and immiscibility with water. This formulation is specifically designed to stain microplastics directly in aquatic environments, exploiting n-heptane's hydrophobic properties to selectively interact with microplastic particles without dissolving in the aqueous phase.

This specificity is crucial because Nile Red selectively stains non-polar microplastics, and n-heptane does not dissolve polar organic substances which could interfere with fluorescence (Datta et al., 1997). We then prepared the NR-H solution in various concentrations of n-heptane, ranging from 3 to 100 mg/L, using the stock solution, aiming to optimize the conditions for the best fluorometric response. This mixture was mechanically agitated in a laboratory flask to ensure thorough staining of microplastics during vortexing. To ensure stable excitation-emission readings, samples were maintained at a constant temperature of 22°C.

Visually, the NR-H dye solution varies in color from yellow-greened to orange. Upon excitation, it emits light in the range of approximately 564 to 600 nm, presenting an orange hue. This shift allows us to choose optimal excitation and emission wavelengths for rapid and precise MNP identification, minimizing interference and quenching in the fluorescence process, presenting characteristics ideally suited for a specially designed submersible fluorometer sensor aimed for detecting colored MNPs (Prata, 2023).

To identify the excitation and emission wavelengths of the NR-Heptane dyes, we employed a SAFAS Xenius XC Spectro fluorescence instrument. NR-H dye solutions and aqueous samples of MNPs tagged with NR-H dye was introduced into quartz cuvettes for the measurements. Ultra-filtered water served as blank for these experiments. Excitation was configured to range from 240–800 nm, incremented by 1 nm, while detection spanned 245–828 nm, also incremented by 1 nm, with an integration time set at 0.01 seconds. Fig. 2 shows the excitation and emission spectra for NR solutions in heptane at different concentrations.

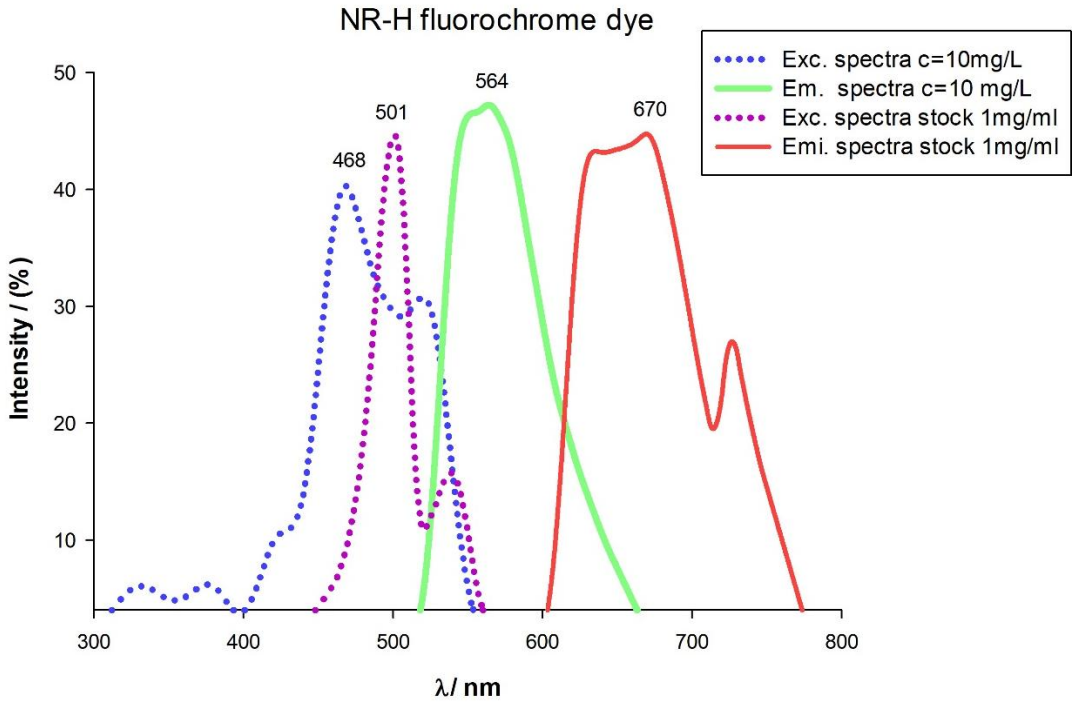

204

205 **Fig. 2.** Plot of the excitation and emission spectra for a stock solution of Nile Red in acetone. Additionally, it
206 includes spectra for its diluted in n-heptane, with concentration of 10 mg/L.

207 *2.4. Natural water sources*

208 Various natural water samples, rich in organic and inorganic solutes, were sourced from
209 locations in the South of France. These aqueous samples were then combined with secondary
210 micro/nano plastics and with primary latex beds.

211 Three differently contaminated water sources were considered:

212 - Firstly, water sample were procured from the wastewater treatment plant (WWTP)
213 located at Rouquet, Agen, France. Two different sampling from such plant were
214 considered: firstly, effluents drawn from the final stage of primary treatment,
215 particularly post the first clarifier phase; the second sampling stems from the secondary
216 treatment's subsequent clarifier step.

- Secondly, groundwater sampling from a place very close to the same WWTP, with a borehole reaching 120 meters length, which reaches the Garonne River phreatic aquifer. This location is aimed for monitoring of potential influences from the WWTP on groundwater quality.
- Finally, seawater samples collected from the surface layer approximately 5 meters off the Montpellier beach in France. The collected water was carefully transferred to 2-liter glass bottles, which were securely sealed with blue caps. These samples were promptly transported to the laboratory to ensure integrity and freshness. During the collection process, both the temperature and salinity of the seawater were recorded using a mercury thermometer and an ATAGO-USA R-5000 refractometer, respectively.
- For the sake of comparison with seawater samples, it was prepared synthesized Seawater (International, 2013). Initiating with a liter of ultrapure water in a beaker, adequate quantities of salts were introduced to replicate seawater's typical ionic composition. These included: Sodium chloride (~23.93g), Magnesium chloride (~5.20g), Magnesium sulfate (~4.09g), Calcium chloride (~1.16g), Potassium chloride (~0.66g), Sodium bicarbonate (~0.10g), and Strontium chloride less than 0.05g. All chemicals were supplied by Themo Fischer (purity > 98%) and used without further purification. For optimal dissolution of the salts, we employed a magnetic stirrer. The solution's pH was subsequently verified and adjusted to fall within the natural seawater range of 7.5 to 8.5. Once all the salts are completely dissolved and the solution is thoroughly mixed, the synthesized seawater was transferred to a storage jug or container. Resulting synthetic seawater only differs from natural one in the absence of organic matter.

The main analytical parameters of all 5 five water samples, including Suspended Solids (SS), Chemical Oxygen Demand (COD), Ammonium (NH4) and turbidity and salinity, were monitored over a 1-month period. Resulting range of values are presented in Table 1.

Table 1: Analytical parameters of the water sources used for testing of MNP's dyeing.

Water Types	Suspended solids (mg/l)	COD (mg/L)	NH4 (mgN/l)	Turbidity (NTU)	Salinity (g/L)
Primary raw water	220-350	600-863	50-75	~103	< 5
Secondary Raw water	21-42	18-63	11	< 5	< 5
Borehole water	< 5	< 20	–	<1	<5
Sea Water	1-7	< 5	–	~2-3	~38
Synthesize Sea water	<1	<1	–	<1	~31

2.5. MNP's staining in water

Primary MNP´s (latex particles) were initially subjected to gentle agitation, after which they were meticulously diluted in deionized water. This dilution process was carefully adjusted to attain a final volume within the range of 250 to 500 milliliters in a glass flask, several drops that was determined by the respective particle diameter. Following the dilution, we administered a gentle ultrasonic treatment for the duration of one hour, a crucial step to ensure the thorough and homogeneous dispersion of the particles. The concentration of these latex particles in relation to the volume dispensed, and across the spectrum of diameters, was quantified. The number of particles per milliliter (Np) was calculated employing a formula

provided by the manufacturer, facilitating an accurate and reproducible measurement of particle concentration.

$$Np = \frac{Wv(\%)\ 6 \cdot 10^{10}}{\pi \rho d^3} \qquad Eq.1$$

where Wv is the percentage of solid polymer (%), which represents the concentration of latex beads, denotes the polymer density (in g/cm³), and d is the particle size (in µm). This equation simplifies to $1.828 \cdot 10^{10}/d^3$ particles, according to manufacturer.

Regarding secondary MNP´s, the degraded mixture (soup) coming from the 5 L bottle was agitated to ensure homogeneity, and then filtered through a 100 µm membrane, to avoid particles over eth Microplastics definition, (Sorensen & Jovanović, 2021).

For dye staining efficacy validation, a 50 ml aliquot composed of 25 ml of water (ultrapure or natural, depending) along with 25 ml of solution containing the corresponding MNP´s (dissolved latex particles or prefiltered soup), housed in a glass centrifuge flask, was employed. The dyeing capability of the NR-H dye was gauged by administering varying volumes, from 0.1 to 10 ml, via an analytical micropipette. After dye application, the microplastics in the sample were subjected to vortex agitation for a total of 40 min, segmented into 10-minute intervals. All aqueous suspensions, whether of MNP's-Lab (secondary) or unidimensional latex beads (primary), once treated with the NR-H dye fluorochrome, were incubated in an oven set at 40°C, selected to avoid higher temperatures affecting the fluorescence intensity (Wang et al., 2021). The procedure was designed to allow any remaining dye (not used in MNP´s staining) to settle on the surface of the water, and a period of 24 h was allocated to ensure the thorough drying of the upper phase, which primarily consisted of n-Heptane.

The final step involves filtering selected samples through a cellulose nitrate (CN) membrane in preparation for further analysis by an optical microscope, which aims to identify colored MNP's in the water. To assure MNP´s retention, the mean pore size of the membranes was selected to be lower than expected particle size. Post-filtration, membranes were preserved in glass Petri dishes and dried in an oven (max. temperature 35 ºC) prior to analysis.

2.6. Staining validation

To validate the staining results, especially regarding the structural adsorption of the fluorochrome onto the latex beads, we conducted additional tests using Scanning Electron Microscopy (SEM), Optical Microscopy and Dynamic Light Scattering (DLS). A Hitachi (T3000) SEM device was used working at resolutions around 0,1 μm, enough for a distinctive view of the involved particles. While an Optical microscope (Tech Systems Loupe Microscope) equipped with a digital camera SONY XCD-U100CR, was also used. The microscope, combined with the camera, provided magnifications ranging from 4x to 20x which results in a minimal resolution of roughly 1 μm/pixel on the resulting images.

Samples before and after MNPs staining were observed with Visible Light and UV Light:

- For Visible light, the primary light source for our observations was a white LED source, whose intensity was finely controlled using advanced photonics optics. Exposure time was set to approximately 40 milliseconds.

- While, in the case of UV Light observation, sample was illuminated by a UV lamp (wavelength 340 nm). Exposure time was now adjusted between 300 to 600 milliseconds, ensuring optimal visualization.

Following visualization, the captured images underwent processing using Filtrex 12.4.0 software, aimed for improving image quality and contrast. In particular, for UV illuminated images, a consistent white background was utilized, crucial in aiding clear visualization. To

ensure precise color representation in the images, chromatic balance adjustments were meticulously conducted.

Dynamic Light Scattering (DLS) technique was applied to measure the diameters of the latex beads pre- and post-staining. For such, a Zetasizer NanoZS from Malvern Analytical was used. 50 ml of distilled water were added to 2 drops of latex particles (0.05 or 0.1µm, while in the case of 0.8 µm beads, 12 drops were added). Dimensions of these beads were measured with DLS prior to staining protocol. Similarly, after the staining process using NR-H dye (see protocol in section 2.5) DLS was used again to measure the diameters of the beads post-staining.

2.7. Submersible fluorometer

A submersible fluorometer, Cyclops 7F, (Turner Designs, San Jose, CA, USA), tailored for lab-based fluorochrome experiments was used in our experiments. It was specifically designed to work in a 400 to 790 nm (with a maximum of Excitation around 460 nm and a maximum of Emission centered on 590 nm), aligning with the excitation-emission spectra of the fluorochrome-NR-H staining shown in Fig. 2. This customization allows the Cyclops 7F to be more effective in the analysis of dyed MNPs. As Turner Designs was asked to supply a special Fluorometer working in a different range from those normally marketed, the company was unable to supply a calibration curve, so the first step was to calibrate the response of the equipment to the presence of Nile Red. For this purpose, a mixture of Nile Red and ethanol (NR-E) was used. This choice was made to tailor the excitation and emission wavelengths to those of Nile Red, while also opting for ethanol as a solvent over acetone to represent the linear response of the device under a fluorescent solvent. Calibration was don dissolving NR powder in ethanol, to get the desired concentration, began with the highest one (100 parts per billion (ppb)) and progressively reducing to as low as 0.2 ppb, closely approaching the instrument's resolution limit. This stepwise approach ensured a thorough calibration across a range of

concentrations, establishing the fluorometer's accuracy and linearity in detecting fluorescent substances.

Once the response of the equipment to the presence of NR was assured, calibrated latex particles (stained using NR-H) were used to evaluate the possibility of using fluorescence measurements to determine the concentration of MNPs (primary in this case). The experimental setup consisted of a non-fluorescent container, specifically a 500 ml glass beaker, placed on a non-reflective black surface. This arrangement ensures that the sensor is positioned centrally in the container, maintaining more than 3 inches above the bottom and at least 2 inches away from the inner circumference of the beaker. Baseline calibration was done with the Cyclops 7F fluorometer submerged in ultra-pure water. The study was conducted thorough measurements on a range of latex beads to guarantee the accuracy and consistency of the results.

3. Results and discussion

3.1. Optimum staining conditions

Optimal staining conditions for micro and nanoplastics (MNPs) in water are essential for their detection. Once our selection was Nile Red, previously dissolved in acetone and then, addition of n-Heptane (NR-H), the first step was to determine the optimal concentration of n-heptane which guarantees clear and distinguishable staining.

Next figure, Fig. 3, represents the emission spectra obtained with Spectro fluorescence. Same volumes of secondary MNP´s, pre-filtered through a 100µm membrane, were subjected to the previously commented staining protocol with NR-H solutions at different n-Heptane concentrations and the excitation (not represented here) and emission spectra of these stained MNP´s samples were studied in the visible range of 400-800 nm. The line marked as c = 0 corresponds to the spectrum obtained with NR only dissolved in acetone (what we have named stock solution).

Using Nile Red in acetone without n-Heptane (c = 0 in the figure), despite achieving high emission intensities and a notable shift towards longer wavelengths due to solvent polarity, resulted in solution precipitation and non-selective water staining, then making it difficult to identify MNPs.

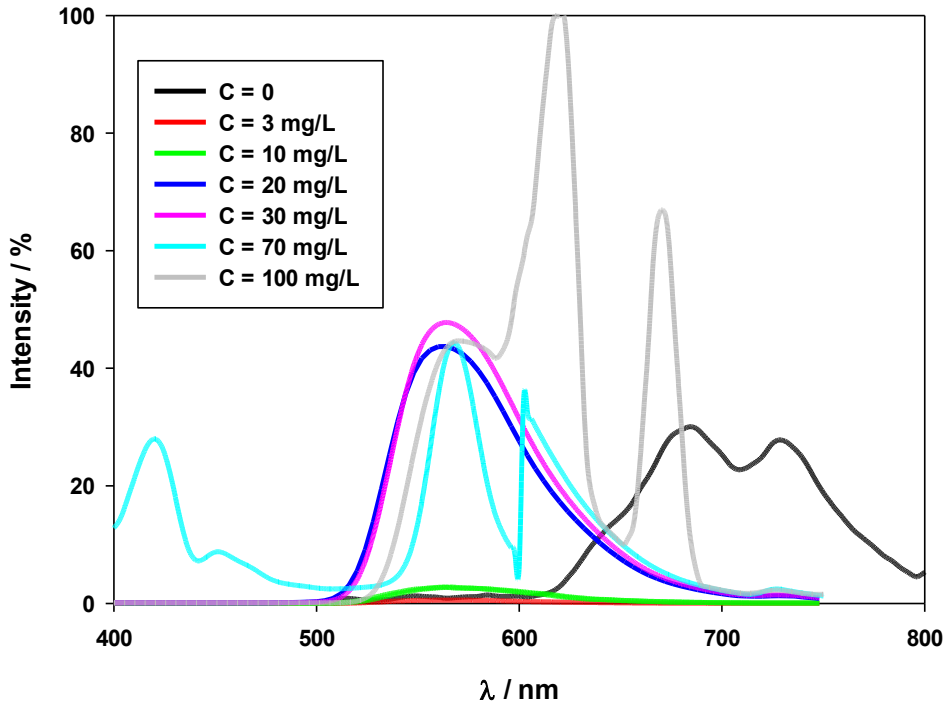

Fig. 3. Dependence of the fluorescence emission signal with the concentration of n-Heptane added to the acetone solution of NR dye.

On the other side, it was found that gradually increasing n-Heptane's (a non-polar solvent) concentration, within the Nile Red dye solution, markedly improved the fluorescence emission peaks. Moreover, the emission spectra in the presence of n-Heptane, moved to a single peak around 560-570 nm. This enhancement was especially evident within the 20 to 70 mg/L concentration range for n-Heptane. Here, we noted a stable and marked rise in emission intensity, signifying the dye's effective microplastic staining. This consistency implies that the Nile Red dye achieves optimal interaction with microplastics in this concentration window, yielding a robust and reliable fluorescence signal.

However, when n-Heptane concentration arrived (and eventually surpassed) 70 mg/L, the emission spectrum's clarity and definition began to degrade, with the spectrum showing distortion and the absence of a distinct peak. This distortion (clearly seen in the results for c = 100 mg/L) suggests that at elevated n-Heptane levels, the solvent's impact on the interaction between dye, plastic, and water might disrupt the fluorescent behavior of Nile Red. This disruption could stem from alterations in the solvent environment surrounding the dye molecules, impacting their capacity to adhere to or interact with microplastic surfaces, thereby modifying the fluorescence characteristics. This observation highlights the critical need to meticulously regulate n-Heptane concentrations to optimize the staining and visualization of Micro-Nano Plastics (MNPs). In our work, a n-Heptane concentration of 20 mg/L was considered optimal as giving maximum single peak fluorescence by using minimum amount of n-Heptane.*3.2. Preliminary results of MNPs (primary and secondary) in ultra-pure water*

Directly staining conditions are crucial for the effective detection and analysis of micro and nanoplastics (MNPs) in water, given the pervasive nature of these contaminants in aquatic environments. Both naturally degraded polystyrene (PS) beads and polyethylene terephthalate (PET) particles coming from the also degraded bottle, fluoresced near orange wavelengths, with particles over 40-50 μm visible to the naked eye. Similarly, latex microbeads in variable concentrations (~10^2 to 10^{12} particles/ml) showed distinct orange staining, visible without magnification, indicating the protocol's effectiveness for various plastic types and concentrations. These features are clearly seen in Fig. 4.

In that figure there are presented both primary and secondary MNP´s before (A and C) and after (B and D) staining. In both cases, stained solutions present clearly distinguishable MNP´s particles, when illuminated with UV light.

To continue with this study of MNP´s staining, both latex bead samples, varying in size from 0.05 μm to 100 μm and immersed in an aqueous medium, and also MNPs generated by long-

term PS and PET degradation, underwent an extensive examination using SEM. The primary focus of this in-depth analysis was to evaluate any potential defects or irregularities in the fluorochrome's adhesion to the bead surfaces, to validate the efficacy of the staining process across the range of bead sizes.

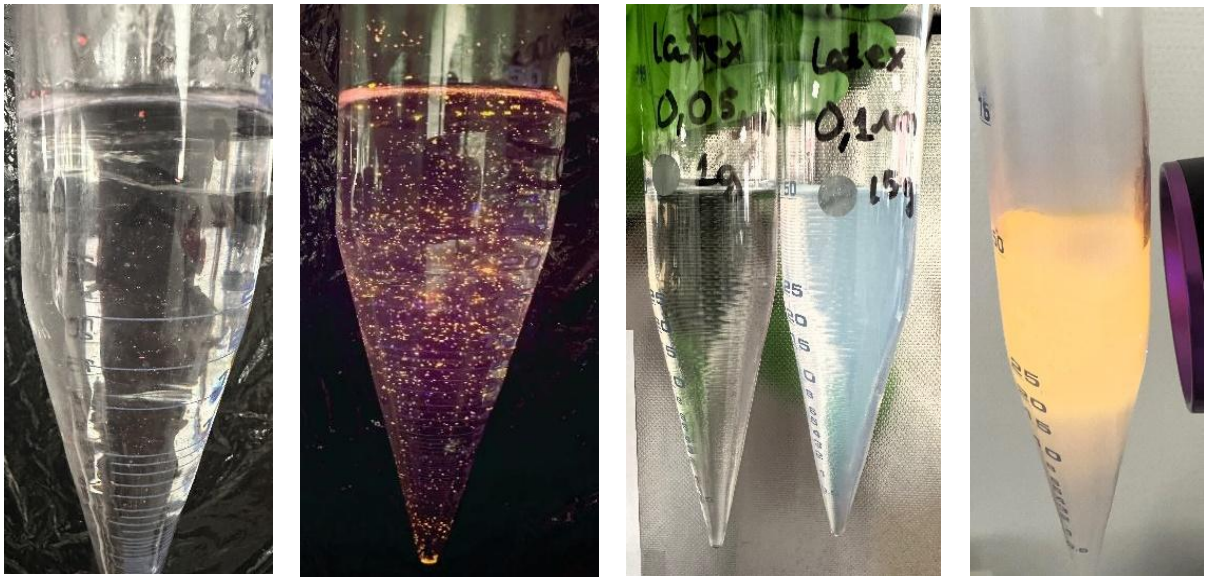

Fig. 4. Several images of MNPs and latex beads: A) Secondary PS and PET MNPs (previously filtered) ranging from 100 to 10µm, suspended in 50 ml of ultra-pure water and viewed under visible light. B) Secondary MNPs stained with NR-H fluorescent dye, in an aqueous solution, examined under UV light (wavelength 365 nm). C) A suspension containing 1 drop of 0.05 µm (left) and 10 drops of 0.1µm (right) latex beads (primary nanoplastics) in 50 ml of ultra-pure water. D) Fluorescently stained latex beads, size 0.05 µm, in an aqueous medium and observed under a 365 nm UV light.

For this visualization, secondary MNP´s and latex of different mean sizes were filtered through adequate size CN membranes (mean pore size lower than particles), so that the particles retained in the membrane surface can be observed in SEM pictures of such membranes. Some of the SEM pictures obtained are presented in Fig. 5. For all pictures presented in that figure, diameters and main dimensions of a representative amount of the visible particles has been determined.

405 Regarding the pictures showing latex beds (5A-C), it should be noted the almost perfect
406 spherical shape they show. But most important, the diameters measured on selected spots in the
407 figures, coincide appreciably with the original size of the latex beads, as certified by NIST, but
408 also checked in corresponding SEM images before NR-H staining (not shown here). Therefore,
409 this collection of SEM images not only emphasizes the diverse size ranges of latex beads but

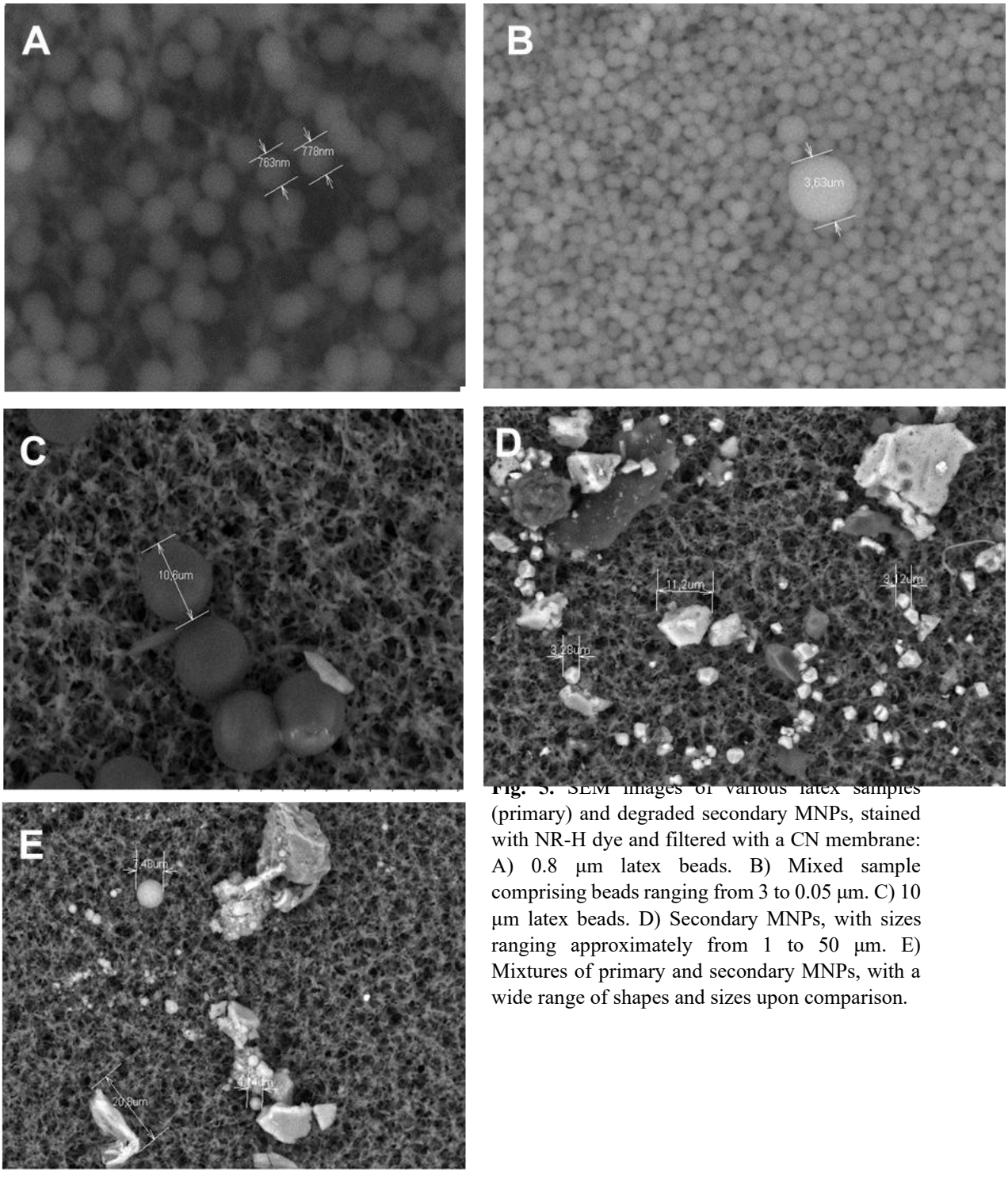

Fig. 5. SEM images of various latex samples (primary) and degraded secondary MNPs, stained with NR-H dye and filtered with a CN membrane: A) 0.8 µm latex beads. B) Mixed sample comprising beads ranging from 3 to 0.05 µm. C) 10 µm latex beads. D) Secondary MNPs, with sizes ranging approximately from 1 to 50 µm. E) Mixtures of primary and secondary MNPs, with a wide range of shapes and sizes upon comparison.

410 also demonstrates that their distinct size characteristics are preserved post-staining with NR-H
411 dye. This series of SEM images confirms that the NR-H dye staining process does not alter the
412 inherent characteristics of the latex beads, even when examined under high-resolution
413 microscopic observation.

414 Similar results were observed for secondary MNPs, see Fig. 5D-E. According to these SEM
415 images, secondary MNPs present a broad distribution of sizes and strong irregularity in their
416 shape. This is clearly expected from the different degree of degradation each particle has
417 achieved through the 1-year period. On the other side, SEM is not able to distinguish which
418 MNPs pieces come from PS pearls, and which are added by the PET bottle degradation.
419 Obviously, in this case, there is no possible to compare the sizes of the particles before and after
420 staining.

421 Complementing the SEM pictures, DLS was also employed for testing latex beads staining. To
422 stabilize the particles and reduce aggregation, some drops of a NaCl suspension (15 g/L) were
423 added to the latex samples. Results of DLS for some latex particles, before and after staining
424 are shown in Fig. 6. The analysis consistently indicates uniform size distribution of the
425 calibrated spheres, as evidenced by their almost overlapping positions on the graph, confirming
426 that the adopted dye-staining method does not significantly alter particle diameter, underscoring
427 its efficacy. From those results, seems clear that NR-H dye doesn't notably alter the bead's
428 diameter. DLS resolution limit was set at 0.3 μm, since the measurement of beads with smaller
429 diameters, less than 0.05μm encounters challenges.

430 DLS was also used in the analysis of secondary MNPs, but results (not shown here) were
431 strongly worse, due to the broad range of particle diameters of these MNP´s inherent to their
432 degradation process, which leads DLS to difficulties in obtaining a particle size distribution.

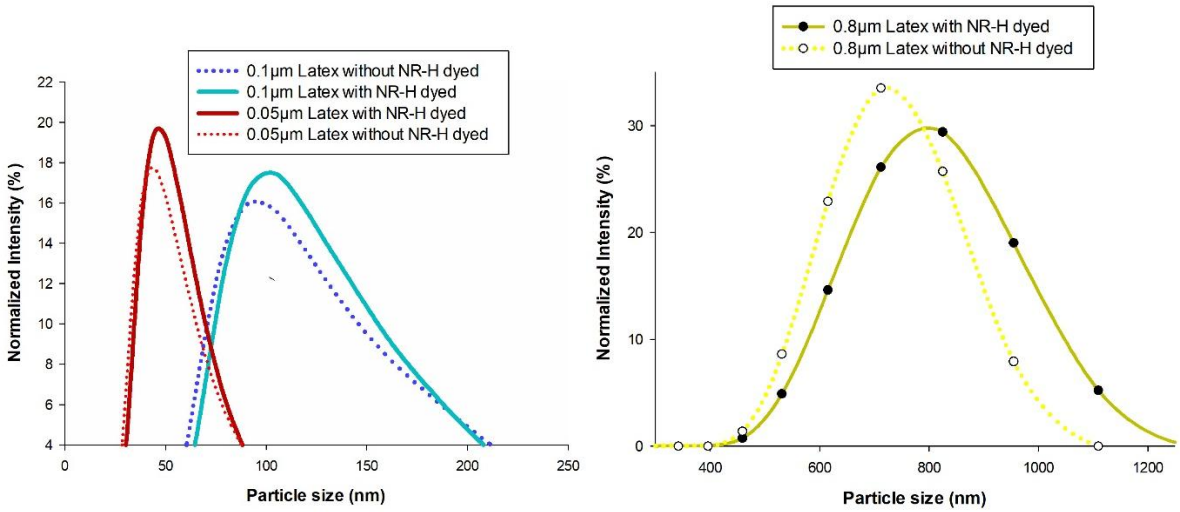

433

434 **Fig. 6.** Results of Dynamic Light Scattering (DLS) Analysis on latex particles. (a) Left figure shows latex beads
435 with diameters of 0.05 µm and 0.1 µm, depicted before and after dyeing, respectively; (b) Right side corresponds
436 to latex beads of 0.8 µm diameter, also before and after the application of dye. The dyeing process here includes
437 the addition of 2 drops of NaCl solution for each measurement, to assure that latex particles do not coagulate.

438 *3.2. Preliminary results of MNP´s in several water sources.*

439 In experiments aimed at evaluating the dyeing efficiency of NR-H in natural conditions,
440 samples were prepared by combining primary and secondary MNPs (previously mixed) with
441 raw WWTP, borehole, sea, and synthetic salted water. Then fluorochrome dye (prepared in the
442 yet commented manner) was added at such solutions in amounts varying between 1 ml to 10
443 ml (depending on the water source turbidity). Each sample was agitated using a vortex mixer.
444 After vigorous mixing, the samples were oven-dried to remove excess dye, so enhancing MNP
445 visibility in various water samples.

446 Examples of the resulting MNPs solutions are shown in Fig. 7 for two water sources coming
447 from a WTTP. In both pictures, stained MNPs are clearly visible as orange spots when
448 illuminated with UV light. They are clearly distinguishable from the blue ground of the water.
449 This blue color is due to the presence of Chromophore Dissolved Organic Matter (CDOM), a
450 group of organic molecules present in water, arising from decaying plant and animal materials,

with a significant contribution from tannins and lignins released during plant decomposition. CDOM re-emits ultraviolet light as visible blue light (approximately 450 to 495 nm). While, NR-H dye, emits primarily in the orange wavelength range, around 540-580 nm, clearly distinguishable from CDOM contribution.

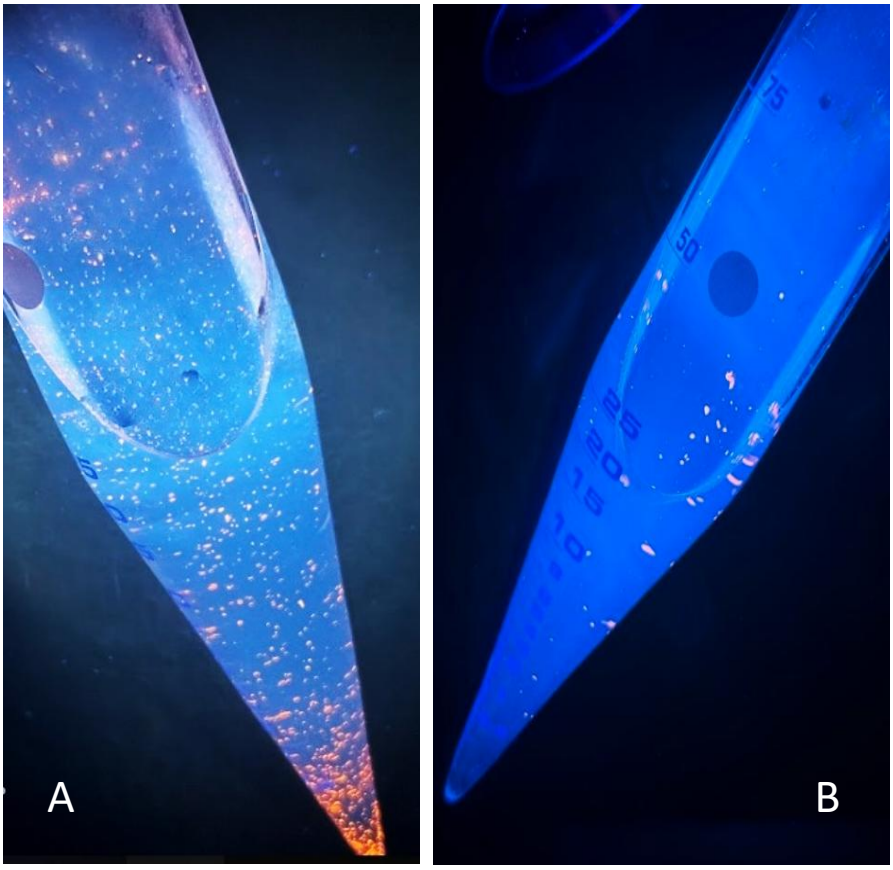

Fig. 7. (a) MNPs fluorescence in WWTP inlet water (Primary raw), illuminated under UV light. (b) Similar image from secondary raw water treatment.

Therefore, from Fig. 7, we can conclude that the NR-H dye is effective on staining the surfaces of primary and secondary plastic fragments in water containing, presumably, a high concentration of suspended organic matter. However, as pointed out by Shim et al, (Shim et al., 2016), some limitations of NR staining, should be considered. Mainly they found that NR can lead to co-staining of organic matter contained in the natural samples. Shim et al. postulated it is needed, in that case, a previous sample treatment to remove lipids and other organic matter.

Certainly, this is a potential limitation to an accurate MNPs staining. In our work, natural samples were mixed with selected concentration of our primary and secondary MNPs, leading to the fluorescence patterns showed in Fig. 7. Nevertheless, when these natural water samples were NR-H stained and then UV illuminated before addition of generated MNPs or latex beads, it was not found any orange spot, that could be result of organic matter staining. Only the already mentioned blue background caused by CDOM, but clearly distinguishable from the orange color of the plastic particles. Anyway, a better understanding of these possible interactions (especially in contexts with abundant organic matter) should be crucial for refining environmental monitoring technique and achieving an accurate method of identification of plastic pollution in aquatic environments.

In both natural and synthesized seawater samples, as well as borehole water, the same staining protocol was applied, resulting in similarly visible fluorescent particles.

To conclude the study of dye adhesion, samples were observed by Optical microscopy. Representative pictures of such observations are included in Table 2, for both Visual and UV illumination of stained microplastics. The images depict a composite of primary and secondary micro- and nanoplastics that have been filtered using a 5 μm cellulose nitrate membrane, which serves as the backdrop in the photographs.

Table 2. Visible (left) and UV (right) optical microscopy images of different origin waters containing a mixture of latex beds and degraded MNPs, once stained with NR-H dye (C=20 mg/L).

WATER TYPE	VIS Observation	UV Observation
Primary raw water	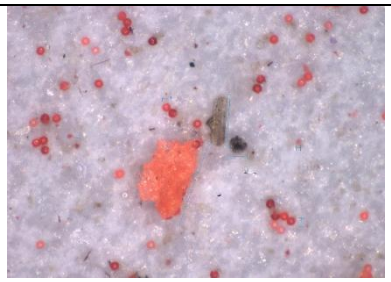	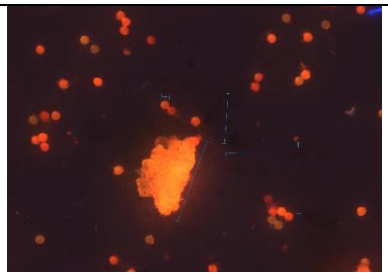
Secondary raw water		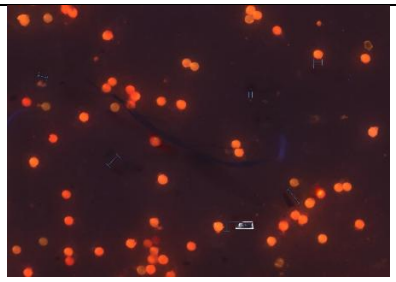
	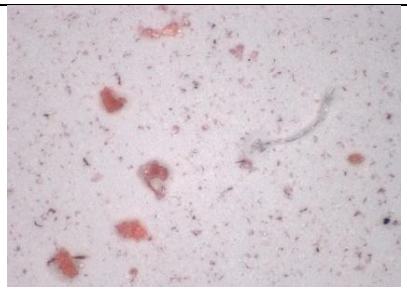	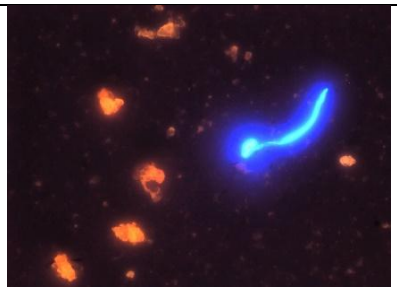
Borehole water	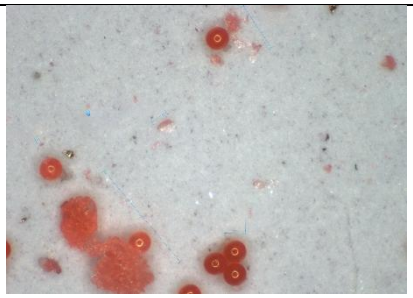	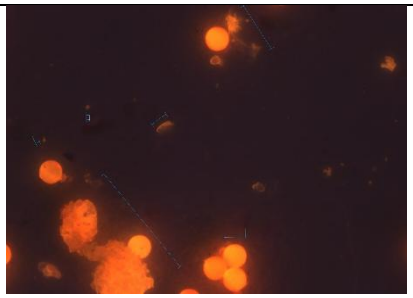

Sea water	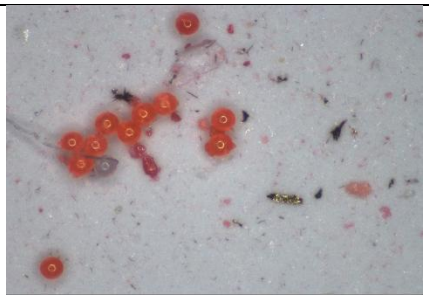	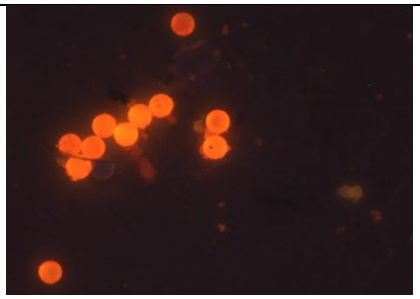
Synthesized sea water	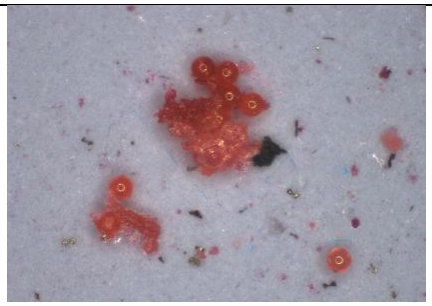	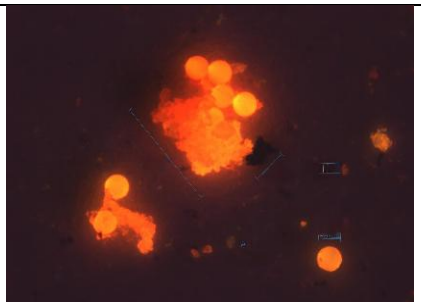

498

499 In the pictures can be easily distinguished the latex particles (almost perfect spheres) in light
500 red color (visible) or clearly orange (UV). Along with, some secondary MPs can be observed,
501 whose main distinctive characteristic is a highly irregular shape (see, for example, primary
502 raw water or borehole water pictures). In the water samples, other components such as metal
503 particles and organic matter remain unstained and appear as more or less black spots under
504 visible light and organic fibers are distinctly observable in blue color when viewed under UV
505 light.

506 Certainly, not all latex particles, and surely not all secondary MNPs exhibit a complete, high-
507 intensity, staining. This phenomenon can be attributed to insufficient dye volume for smaller
508 diameter beads or irregular shape for secondary ones, suggesting a correlation, worthy of study,
509 between bead size and staining efficiency. So, the wide variation in size might affect the
510 uniformity of the staining process. Secondly, there might be limitations in the dyeing process
511 when it comes to irregularly shaped or fractal parts of secondary MNPs, particularly those
512 smaller than 1μm. These particles, due to their unique shapes and sizes, may not absorb the dye

as effectively as more uniformly shaped particles, leading to less pronounced or uneven staining. Nevertheless, it appears as even for highly irregular particles, there is a substantial part of them correctly stained, enough to clearly detect such particles in the water source. Additionally, our observations reveal significant some trend to form agglomerations between primary and MNPs (see borehole and synthetized sea water pictures, for example), indicative of complex interactions within the aquatic environment.

This aspect of our research indicates a need for further investigation. Future studies should focus on refining the staining process for secondary MNPs, especially for those with complex shapes and smaller sizes (Stanton et al., 2019). Such research could involve developing more advanced or targeted staining techniques that can more effectively and uniformly dye MNPs of various shapes and sizes. By addressing these potential limitations, we aim to enhance the accuracy and consistency of our methodology for detecting and analyzing primary MNPs, contributing to a deeper understanding of their characteristics and behavior in various environments.

3.3. Preliminary results of fluorescence spectroscopy and fluorometry in secondary MNPs

We employed the SAFAS Xenius XC Spectrofluorometer to measure the fluorescence intensity of stock solutions containing secondary microplastics, which had been filtered through a 50 µm filter prior to analysis. These stock solutions were subjected to a series of 2-fold dilutions, ranging from the undiluted stock solution (n=0) to a 1/1024 dilution (n=10). Fluorescence spectra for each dilution were recorded, as shown in Figure 8.

Key Observations:

1. Intensity-Dependent Quantification: *The fluorescence intensity systematically decreased with increasing dilution, demonstrating a clear correlation between microplastic concentration and fluorescence signal intensity. The highest fluorescence*

intensity was observed in the undiluted stock solution, with progressively lower intensities in the diluted samples.

2. Effective Detection Range: *The spectrofluorometer effectively detected microplastics across a wide concentration range. The solvatochromic effect of NR caused a shift of the fluorescence towards higher wavelengths with increasing polarity of the polymers (e.g., PS and PET), due to binding to the particle surface or incorporation into the polymeric network (Sturm et al., 2021). The distinct peaks observed around 600 nm correspond to the fluorescence emission of the NR-H dye bound to the microplastics, indicating successful staining and detection.*

3. Consistency and Accuracy*: The consistency of the fluorescence peaks across different dilutions underscores the reliability of the NR-H staining protocol and the accuracy of the spectrofluorometer calibration. This reliability is crucial for the accurate quantification and characterization of microplastics in various aqueous media.*

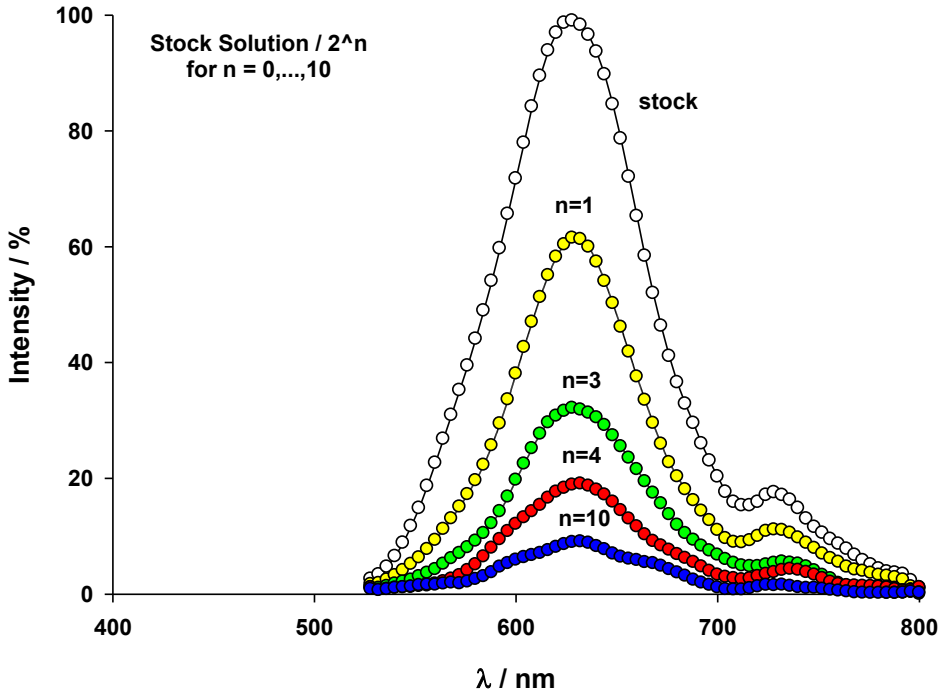

Fig. 8. Observation of secondary MNPs by using the Cyclops 7F fluorometer. The resulting signal reading is shown in the device screen.

As part of our protocol validation, we conducted a calibration test on the Cyclops 7F fluorometer to ensure its accurate response within the desired wavelength range of 400 to 790 nm. This calibration meticulously covered concentrations from 100 parts per billion (ppb) down to 0.1 ppb, near the instrument's resolution threshold. The resulting calibration curve demonstrated a distinct linear relationship between the concentration of the NR-H mixture and the fluorometer's voltage readings, expressed in millivolts (mV), with a correlation coefficient of 0.999, affirming the reliability of our measurements.

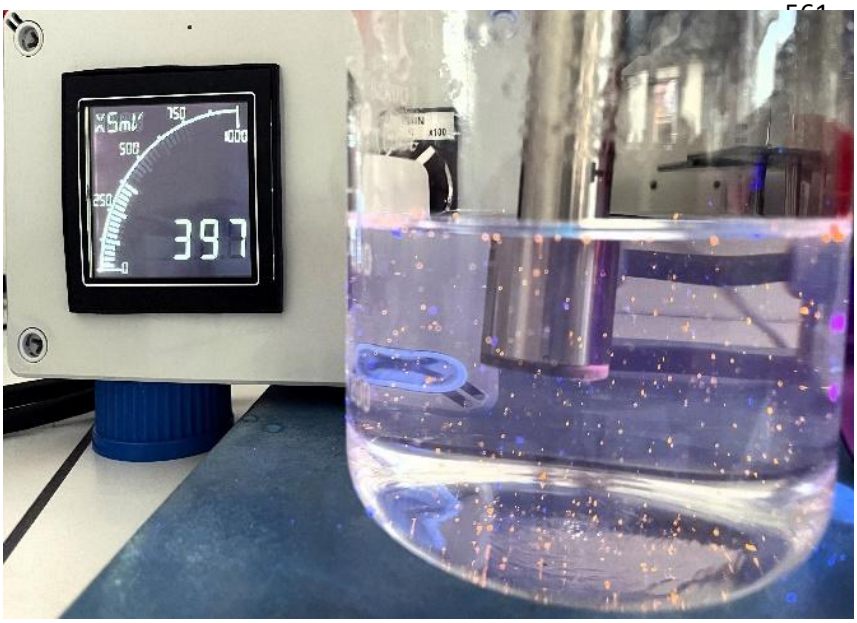

Fig. 9. Observation of secondary MNPs by using the Cyclops 7F fluorometer. The resulting signal reading is shown in the device screen.

Once the linear response of the fluorometer was demonstrated, we tested its utility in detecting MNPs in aqueous media. Fig. 9 illustrates the setup for fluorometer measurements, with the Cyclops 7F fluorometer immersed in a glass beaker containing the water sample to which

573 secondary MNPs had been added. The fluorometer screen showed that the technique is sensitive
574 to the presence of MNPs in the water, resulting in appreciable signal readings.

575 Despite its sensitivity to NR-H, the technique does not allow for discrimination of the
576 concentration or origin of secondary MNPs (i.e., whether particles originate from PS beads or
577 PET bottles). However, the presented protocol ensures the presence of MNPs in suspected
578 contaminated water sources without the need for pre-treatment to remove substances that may
579 lead to false positives.

580 The systematic decrease in fluorescence intensity with dilution confirms that our staining
581 protocol, combined with the Cyclops 7F submersible fluorometer, provides a robust method for
582 quantifying secondary microplastics based on fluorescence intensity. The method's sensitivity
583 and dynamic range are validated by the clear, consistent peaks observed in the spectra.

584 These results validate the efficacy of our NR-H staining protocol and the spectrofluorometric
585 detection method, providing a reliable approach for the identification and quantification of
586 secondary microplastics in environmental water samples. Future work will focus on refining
587 this method to enhance specificity and sensitivity, as well as adapting it to a broader range of
588 polymer types and environmental conditions.

589 *3.4. Preliminary results of fluorometry in primary MNPs*

590 As for primary MNPs, taking advantage of the fact that particles of very well-defined sizes are
591 available, a study of the fluorometer response to NR-H stained latex beds was carried out. For
592 this purpose, the response to different concentrations of latex particles of different sizes was
593 measured. Fig. 10 shows these fluorometric signal measurements for various latex sizes (10,
594 0.5 and 0.05 μm). These results are presented in double logarithmic scale, where the
595 concentrations have been translated into number of particles present by using equation (1). It
596 can be seen how, for each latex particle size, there is a clear linearity, which translates into an

increase in the detected signal as the number of particles present increases. These plots could be used as a calibration curve to determine the concentration of particles in each sample assuming that only particles of a single size are present.

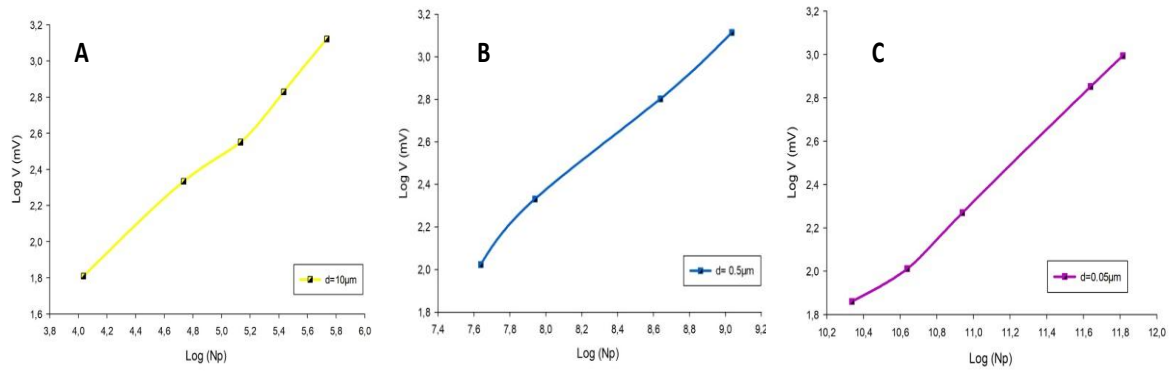

Fig. 10. Double logarithmic plot of the fluorometer response vs the number of latex particles for different latex sizes (A: 10 µm; B: 0.5 µm; C: 0.05 µm).

On the other side, when comparing results in plots A, B and C, it is also remarkable (and otherwise expected) that larger particle sizes need less concentration to give a measurable fluorometric signal.

Unfortunately, when dealing with latex beds of different sizes, a single fluorometer reading does not allow us to decide simultaneously on the size and concentration of the particles present. This is clearly seen in the following figure, (Fig. 11) where the response curves of the fluorometer to the different latex particles available are represented. Thus, for a given reading (400 mV = $10^{2.6}$), the graph lacks univocity, so that it could correspond to 10^3 particles of 40 µm, 10^{12} of 0.1 µm, or even to a combination of different quantities from various sized particles.

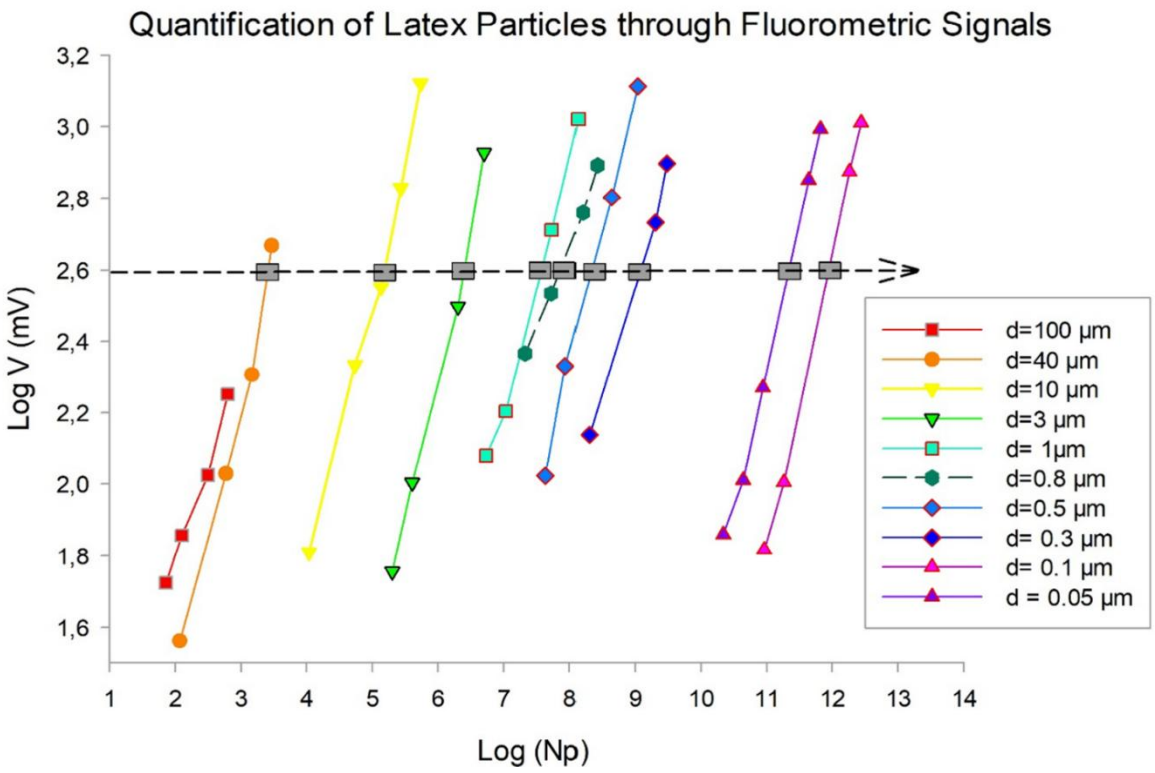

Fig. 11. Quantitative correlation of fluorometric signal intensity (mV) with concentration of latex beads across a spectrum of particle sizes.

Particularly noteworthy is the presence of overlapping data points across different particle sizes, suggesting a limitation in using fluorometry response as a sole metric for determining particle size or concentration.

This limitation can be attributed to the fact that different particle sizes with varying surface areas could adsorb the dye differently, resulting in a similar fluorescence intensity. Consequently, the surface adsorption characteristics of Nile Red may introduce ambiguity in the interpretation of the fluorescence data when used as a standalone method.

In conclusion, while the fluorometric analysis is clearly useful in an initial detection of MNPs presence, its limitations suggest the use of an analytical strategy combining fluorometry with other characterization techniques, like NTA, DLS, SEM or vibrational spectroscopy among others. These methods can offer in-depth insights into the size, shape, and distribution of the particles, providing a more complete picture than fluorometry alone.

4. Conclusion

This study has significantly advanced the detection and characterization of micro- and nano-plastics (MNPs) in various aqueous media. We developed and validated a staining protocol that minimizes pre-processing steps, enabling the direct identification and potential quantification of MNPs in water from multiple sources. The protocol proved effective on both commercially available latex particles with well-defined sizes (primary MNPs) and secondary MNPs created through controlled degradation of common polymers like PS and PET.

The key findings of this research can be summarized as follows:

A) Staining Efficacy: Our direct staining method with NR-H has demonstrated high efficiency in marking MNPs, eliminating traditional sampling and separation processes. It has shown effectiveness in both controlled laboratory conditions and real-world water samples with varying levels of contamination. However, variations in water quality—such as pH, temperature, and ionic strength—significantly influence staining efficiency, indicating the need for further study on these factors.

B) Validation Techniques: The reliability of our staining results has been corroborated through the use of advanced analytical techniques, including Scanning Electron Microscopy (SEM), Dynamic Light Scattering (DLS), and optical microscopy, which have provided precise characterizations of the MNPs.

C) Fluorometric Detection: The Cyclops 7F submersible fluorometer, specially calibrated to align with the NR-H dye, has been instrumental in detecting stained MNPs effectively. This tool's calibrated use, especially with Nile red in ethanol, has confirmed its accuracy and consistency.

D) Quantitative Analysis: Analysis of NR-H stained latex particles has established a linear relationship between particle quantity and detected signal, although distinguishing particle size and concentration in complex mixtures remains challenging.

E) Secondary MNP Detection: While effective in detecting secondary MNPs, their irregular shapes and diverse sizes necessitate the use of additional characterization methods for precise quantification.

We consider the proposed methodology to be a significant step forward in the field, offering a streamlined, cost-effective approach for the rapid identification and characterization of MNPs. This approach is poised to enhance monitoring efforts across various aquatic systems, from oceans to groundwater, supporting interventions to reduce plastic pollution. The potential implications of our findings are vast, affecting environmental monitoring, water treatment processes, marine biodiversity, public health, and industrial practices.

The research presented proposes a rapid and reliable protocol for the identification of MNPs in aqueous samples, fulfilling the initial objectives. However, it also opens new questions and perspectives requiring further investigation. Open areas for future research include:

1. Methodological Extension: Expanding the protocol to include all types of natural samples will allow rigorous testing of the efficacy and robustness of the NR-H staining protocol under real conditions. Collaboration with environmental research groups will facilitate testing in a wide range of contaminated waters, ensuring results accurately reflect various ecological scenarios.

2. Adaptation for Diverse MNP Polymers: Continuing to adapt our staining techniques for various MNP polymer types (primary and secondary) is essential. Our current approach focuses primarily on polar microplastics, and we seek to address a broader spectrum of

polymer chemistries to develop a truly inclusive MNP detection protocol directly in water.

3. Refinement of Quantification Capabilities: Ongoing studies aim to refine the quantification capabilities of our methods and explore the sensitivity limits of our fluorometric techniques for various polymers and concentrations.

4. Addressing Organic Particulate Interference: Addressing organic particulate interference in natural samples remains a key concern. Future research will integrate advanced spectroscopic techniques, such as fluorescence lifetime imaging (FLIM) and hyperspectral imaging, to differentiate MNPs more accurately from background fluorescence. These improvements are expected to significantly increase the specificity of the NR-H staining method, reduce the likelihood of false positives, and improve the reliability of our quantitative analyses.

Acknowledgements

This research was funded by the French Nouvelle Aquitaine Region.

References

Alvim, C. B., Bes-Piá, M. A., Mendoza-Roca, J. A., & Alonso-Molina, J. L. (2023). Identification of microfibers in drinking water with Nile Red. Limitations and strengths. *Journal of Environmental Chemical Engineering*, *11*(3). https://doi.org/10.1016/j.jece.2023.109697

Andrady, A. L. (2011). Microplastics in the marine environment. In *Marine Pollution Bulletin* (Vol. 62, Issue 8). https://doi.org/10.1016/j.marpolbul.2011.05.030

Andrady, A. L. (2017). The plastic in microplastics: A review. In *Marine Pollution Bulletin* (Vol. 119, Issue 1). https://doi.org/10.1016/j.marpolbul.2017.01.082

Bianco, A., Carena, L., Peitsaro, N., Sordello, F., Vione, D., & Passananti, M. (2023). Rapid detection of nanoplastics and small microplastics by Nile-Red staining and flow cytometry. *Environmental Chemistry Letters*, *21*(2). https://doi.org/10.1007/s10311-022-01545-3

Brennholt, N., Heß, M., & Reifferscheid, G. (2018). Freshwater microplastics: Challenges for regulation and management. In *Handbook of Environmental Chemistry* (Vol. 58). https://doi.org/10.1007/978-3-319-61615-5_12

Burzio, C., Ekholm, J., Modin, O., Falås, P., Svahn, O., Persson, F., van Erp, T., Gustavsson, D. J. I., & Wilén, B. M. (2022). Removal of organic micropollutants from municipal wastewater by aerobic granular sludge and conventional activated sludge. *Journal of Hazardous Materials*, *438*. https://doi.org/10.1016/j.jhazmat.2022.129528

Campo, P., Holmes, A., & Coulon, F. (2019). A method for the characterisation of microplastics in sludge. *MethodsX*, *6*. https://doi.org/10.1016/j.mex.2019.11.020

Datta, A., Mandal, D., Pal, S. K., & Bhattacharyya, K. (1997). Intramolecular charge transfer processes in confined systems. Nile red in reverse micelles. *Journal of Physical Chemistry B*, *101*(49). https://doi.org/10.1021/jp971576m

El Hadri, H., Gigault, J., Maxit, B., Grassl, B., & Reynaud, S. (2020). Nanoplastic from mechanically degraded primary and secondary microplastics for environmental assessments. *NanoImpact*, *17*. https://doi.org/10.1016/j.impact.2019.100206

Fan, Y. Van, Jiang, P., Tan, R. R., Aviso, K. B., You, F., Zhao, X., Lee, C. T., & Klemeš, J. J. (2022). Forecasting plastic waste generation and interventions for environmental hazard mitigation. *Journal of Hazardous Materials*, *424*. https://doi.org/10.1016/j.jhazmat.2021.127330

Frias, J. P. G. L., & Nash, R. (2019). Microplastics: Finding a consensus on the definition. *Marine Pollution Bulletin*, *138*. https://doi.org/10.1016/j.marpolbul.2018.11.022

Gagné, F., Auclair, J., & Quinn, B. (2019). Detection of polystyrene nanoplastics in biological samples based on the solvatochromic properties of Nile red: application in Hydra attenuata exposed to nanoplastics. *Environmental Science and Pollution Research*, *26*(32). https://doi.org/10.1007/s11356-019-06501-3

Gonçalves, J. M., & Bebianno, M. J. (2021). Nanoplastics impact on marine biota: A review. *Environmental Pollution*, *273*. https://doi.org/10.1016/j.envpol.2021.116426

Hernandez, L. M., Farner, J. M., Claveau-Mallet, D., Okshevsky, M., Jahandideh, H., Matthews, S., Roy, R., Yaylayan, V., & Tufenkji, N. (2023). Optimizing the Concentration of Nile Red for Screening of Microplastics in Drinking Water. *ACS ES and T Water*, *3*(4). https://doi.org/10.1021/acsestwater.2c00503

Ibrahim, I. A., Rawindran, H., Alam, M. M., Leong, W. H., Sahrin, N. T., Ng, H. S., Chan, Y. J., Abdelfattah, E. A., Lim, J. W., Aliyu, U. S. ad, & Khoo, K. S. (2024). Mitigating persistent organic pollutants from marine plastics through enhanced recycling: A review. In *Environmental Research* (Vol. 240). https://doi.org/10.1016/j.envres.2023.117533

Jiménez-Lamana, J., Gondikas, A., Mattsson, K., & Gigault, J. (2023). Editorial: Analytical methodologies for the analysis and monitoring of nano/microplastics pollution. *Frontiers in Environmental Chemistry*, *4*. https://doi.org/10.3389/fenvc.2023.1191236

Koraltan, İ., Mavruk, S., & Güven, O. (2022). Effect of biological and environmental factors on microplastic ingestion of commercial fish species. *Chemosphere*, *303*. https://doi.org/10.1016/j.chemosphere.2022.135101

Lee, J., & Chae, K. J. (2021). A systematic protocol of microplastics analysis from their identification to quantification in water environment: A comprehensive review. In *Journal of Hazardous Materials* (Vol. 403). https://doi.org/10.1016/j.jhazmat.2020.124049

Maes, T., Jessop, R., Wellner, N., Haupt, K., & Mayes, A. G. (2017). A rapid-screening approach to detect and quantify microplastics based on fluorescent tagging with Nile Red. *Scientific Reports*, *7*. https://doi.org/10.1038/srep44501

Myszograj, M. (2020). Microplastic in Food and Drinking Water - Environmental Monitoring Data. *Civil and Environmental Engineering Reports*, *30*(4). https://doi.org/10.2478/ceer-2020-0060

Nalbone, L., Panebianco, A., Giarratana, F., & Russell, M. (2021). Nile Red staining for detecting microplastics in biota: Preliminary evidence. *Marine Pollution Bulletin*, *172*. https://doi.org/10.1016/j.marpolbul.2021.112888

Pradel, A., Gautier, M., Bavay, D., & Gigault, J. (2022). Correction: Micro- and nanoplastic transfer in freezing saltwater: implications for their fate in polar waters. *Environmental Science: Processes & Impacts*, *24*(1). https://doi.org/10.1039/d1em90040d

Prata, J. C. (2023). Influence of intrinsic plastics characteristics on Nile Red staining and fluorescence. *Journal of Sea Research*, *195*. https://doi.org/10.1016/j.seares.2023.102431

Prata, J. C., Sequeira, I. F., Monteiro, S. S., Silva, A. L. P., da Costa, J. P., Dias-Pereira, P., Fernandes, A. J. S., da Costa, F. M., Duarte, A. C., & Rocha-Santos, T. (2021). Preparation of biological samples for microplastic identification by Nile Red. *Science of the Total Environment*, *783*. https://doi.org/10.1016/j.scitotenv.2021.147065

Rezania, S., Park, J., Md Din, M. F., Mat Taib, S., Talaiekhozani, A., Kumar Yadav, K., & Kamyab, H. (2018). Microplastics pollution in different aquatic environments and biota: A review of recent studies. In *Marine Pollution Bulletin* (Vol. 133). https://doi.org/10.1016/j.marpolbul.2018.05.022

Shim, W. J., Song, Y. K., Hong, S. H., & Jang, M. (2016). Identification and quantification of microplastics using Nile Red staining. *Marine Pollution Bulletin*, *113*(1–2). https://doi.org/10.1016/j.marpolbul.2016.10.049

Shruti, V. C., Pérez-Guevara, F., Elizalde-Martínez, I., & Kutralam-Muniasamy, G. (2021). Toward a unified framework for investigating micro(nano)plastics in packaged beverages intended for human consumption. In *Environmental Pollution* (Vol. 268). https://doi.org/10.1016/j.envpol.2020.115811

Stanton, T., Johnson, M., Nathanail, P., Gomes, R. L., Needham, T., & Burson, A. (2019). Exploring the Efficacy of Nile Red in Microplastic Quantification: A Costaining Approach. *Environmental Science and Technology Letters*, *6*(10). https://doi.org/10.1021/acs.estlett.9b00499

Sturm, M. T., Horn, H., & Schuhen, K. (2021). The potential of fluorescent dyes—comparative study of Nile red and three derivatives for the detection of microplastics. *Analytical and Bioanalytical Chemistry*, *413*(4). https://doi.org/10.1007/s00216-020-03066-w

Sturm, M. T., Myers, E., Schober, D., Korzin, A., & Schuhen, K. (2023). Development of an Inexpensive and Comparable Microplastic Detection Method Using Fluorescent Staining with Novel Nile Red Derivatives. *Analytica*, *4*(1). https://doi.org/10.3390/analytica4010004

Tirkey, A., & Upadhyay, L. S. B. (2021). Microplastics: An overview on separation, identification and characterization of microplastics. In *Marine Pollution Bulletin* (Vol. 170). https://doi.org/10.1016/j.marpolbul.2021.112604

Toussaint, B., Raffael, B., Angers-Loustau, A., Gilliland, D., Kestens, V., Petrillo, M., Rio-Echevarria, I. M., & Van den Eede, G. (2019). Review of micro- and nanoplastic contamination in the food chain. In *Food Additives and Contaminants - Part A Chemistry, Analysis, Control, Exposure and Risk Assessment* (Vol. 36, Issue 5). https://doi.org/10.1080/19440049.2019.1583381

Tröger, R., Klöckner, P., Ahrens, L., & Wiberg, K. (2018). Micropollutants in drinking water from source to tap - Method development and application of a multiresidue screening method. *Science of the Total Environment*, *627*. https://doi.org/10.1016/j.scitotenv.2018.01.277

Wang, C., Jiang, L., Liu, R., He, M., Cui, X., & Wang, C. (2021). Comprehensive assessment of factors influencing Nile red staining: Eliciting solutions for efficient microplastics analysis. *Marine Pollution Bulletin*, *171*. https://doi.org/10.1016/j.marpolbul.2021.112698

Zhang, J., Peng, M., Lian, E., Xia, L., Asimakopoulos, A. G., Luo, S., & Wang, L. (2023). Identification of Poly(ethylene terephthalate) Nanoplastics in Commercially Bottled Drinking Water Using Surface-Enhanced Raman Spectroscopy. *Environmental Science and Technology*, *57*(22). https://doi.org/10.1021/acs.est.3c00842